Supplemental Material

Cell Culture. The renin-expressing As4.1 cell line (ATCC® CRL-2193™), harboring a *Ren2* 5′-flanking sequence/SV40 T antigen hybrid transgene (1) was cultured in high glucose DMEM (Gibco #11965-092), 10% FBS at 37°C in a humidified incubator containing 5% of CO_2.

We used cultured arteriolar smooth muscle cells (SMCs) of the renin lineage that express CFP, a renin lineage marker, and YFP when cells are induced to produce renin (2). This cell line was cultured in DMEM/F12 (Gibco #25300) + 10% FBS, 37°C.

Neutral Red Staining. To visualize renin granules in As4.1 cells were stained with the vital dye Neutral Red (3-amino-7-dimethylamino-2-methyl-phenazine hydrochloride) (Sigma, N4638). The neutral red powder was dissolved in 5ml of DPBS and was used at a final concentration of 100μM in the growth medium. Two hundred thousand cells were plated into a 9.5cm^2 well. The following day, the growth medium was removed and fresh medium/neutral red was added, and cells were incubated for 3hs at 37°C in a humidified incubator containing 5% of CO_2. After the incubation time, the medium containing neutral red was removed, and the cells were washed three times with regular medium and imaged a Leica DMIRE2 microscope.

Animals. To study the juxtaglomerular cells and to perform the acute recruitment study, we used adult *Ren1c*$^{+/+}$*; Ren1*$^{c\text{-}YFP}$ mice. To study the recruited native renin cells we used the *Ren1*$^{c\text{-}/\text{-}}$*; Ren1*$^{c\text{-}YFP}$ mice which were generated by crossing *Ren1*$^{c\text{-}/\text{-}}$ mice described previously (3) with *Ren1*$^{c\text{-}YFP}$ transgenic mice where the expression of YFP is driven by the *Ren1*^{c} promoter, thus marking renin cells (2).

Med1$^{fl/fl}$ mice were obtained from Reddy and Jia's lab from Northwestern University (4). To investigate the function of Mediator subunit 1 in renin-expressing cells we first generated a *Med1*$^{\Delta/+}$ line by crossing *Med1*$^{fl/fl}$ (4) with a mouse expressing *Sox2*^{Cre} to obtain mice harboring one null Med1 allele. After, we bred *Med1*$^{\Delta/\text{-}}$ with *Ren1*$^{dCre/+}$ (5) to generate *Med1*$^{\Delta/+}$*; Ren1*$^{dCre/+}$ mice, which were then bred to *Med1*$^{fl/fl}$ mice to obtain *Med1*$^{fl/\Delta}$*; Ren1*$^{dCre/+}$ conditional knock-out mice and *Med1*$^{fl/\Delta}$*; Ren1*$^{d+/+}$ and *Med1*$^{fl/+}$*; Ren1*$^{dCre/+}$ control mice. All mice were studied at 4-5 months. Mutants n=12 (6 females and 6 males); Controls, n=14 (4 females and 10 males). Males and females were used for this study and because they did not show gender differences, they were grouped to display the data. Of these, six mutant and six control mice were used to measure their blood pressure.

All animals were handled in accordance with the National Institutes of Health guidelines for the care and use of experimental animals, and the study was approved by the Institutional Animal Care and Use Committee of the University of Virginia.

Genotyping. Mouse genotypes from tail biopsies were determined using real-time PCR with specific probes designed to identify the deleted and the wild type allele of *Ren1*$^{-/-}$ as well as the YFP sequence (Transnetyx, Cordova, TN). Genotyping for *Med1*$^{\Delta/fl}$*; Ren1*$^{dCre/+}$ was done using a pair of primers for the wild type and floxed band and another set of primers to detect the deletion band (6).

Renin Cell Isolation. Native Renin cells were isolated from the kidney cortex of adult animals using FACS sorting, utilizing our *Ren1*$^{c\text{-}YFP}$ reporter mice. *Ren1*$^{c\text{-}YFP}$ and *Ren1*$^{c\text{-}/\text{-}}$*; Ren1*$^{c\text{-}YFP}$ mice were anesthetized with tribromoethanol as previously described (7). The kidneys were excised, decapsulated, demedullated, and placed in a 15ml Falcon tube with 2mls of PBS on ice. The kidney cortices from each animal were dissected and placed on a glass slide, minced to a smooth consistency, and transferred into a 15 ml Falcon tube with 5 ml of enzymatic solution [0.3%

collagenase A (Roche, Indianapolis, IN), 0.25% trypsin (Sigma- Aldrich, St. Louis, MO), and 0.0021% DNase I (Roche Applied Science)]. The tubes were placed flat inside a shaking incubator (80 RPM) for 15 minutes at 37°C. Then, the solution was pipetted up/down ten times with a sterile transfer pipette and allowed to settle for 2 minutes, and the supernatant was collected with a plastic pipette and transferred to a fresh 15 ml tube on ice. The enzymatic solution was added to the 15 ml Falcon tube containing the remaining undigested cortices, and the digestion procedure was repeated two more times. The supernatants collected from the three digestions were pooled and centrifuged in a Sorvall RT 6000 Refrigerated Centrifuge at 1,200 *g* for 4 minutes at 4°C. The cell pellet was resuspended with 25 ml of fresh *buffer 1* (130 mM NaCl, 5 mM KCl, 2 mM CaCl2, 10 mM glucose, 20 mM sucrose, 10 mM HEPES, pH 7.4), and the suspension was poured through a sterile 100 μm nylon cell strainer (Falcon™ Cell Strainers, Corning, Inc. 352360) and washed with an additional 3–5 ml of *buffer 1*. The flow-through was poured through a sterile 40 μm nylon cell strainer (Falcon™ Cell Strainers, Corning, Inc. 352340) and washed with 3–5 ml of *buffer 1*. The flow-through was centrifuged at 1,200 *g* for 4 min at 4°C. After the centrifugation, the cell pellet was resuspended in 1ml of *resuspension buffer* [PBS, 1% FBS, 1 mM EDTA, DNAase I (Roche Applied Science)] and analyzed using a fluorescent-activated cell sorter (Influx Cell Sorter).

Chromatin Immunoprecipitation followed by Sequencing. Chromatin immunoprecipitation (ChIP-Seq) was performed by Active Motif (Carlsbad, CA). As4.1 cells were grown to a final count of $1{,}5x10^7$ cells for each ChIP-seq experiment and fixed according to the manufacturer protocol. From $Ren1^{c-/-}$; $Ren1^{c\text{-}YFP}$ mice $1x10^5$ cells were isolated, FAC sorted, snap-frozen in liquid nitrogen and shipped unfixed to Active Motif to perform Low Cell Number ChIP-Seq. Chromatin was precipitated with antibodies against H3K27ac, a marker of active enhancers (AM 39133), Med1, a co-activator (Bethyl Laboratories, cat# A300-793A), RNA Polymerase II phosphoserine 2 (#39097, Clone 4H8, Active Motif), to determine occupancy of RNA Pol II across the genome.

ChIP and Input DNAs were processed into Illumina sequencing libraries, using NextSeq 500. The 75 nt reads generated, were aligned to the mouse genome (mm10) using the BWA algorithm (default settings). Duplicate reads were removed and only uniquely mapped reads (mapping quality >= 25) were used for further analysis. Alignments were extended in silico at their 3'-ends to a length of 200 bp (using Active Motif software), and to identify the density of the extended tags, they were assigned to 32-nt bins along the genome, and the resulting number of fragments in each bin was determined. The resulting histograms of fragments densities (genomic "signal maps") were stored in *.bigWig* files. Peak locations related to H3K27ac and Med1 were determined using the MACS algorithm v1.4.2 (Model-based analysis of ChIP-seq) (8) with a cutoff of *p-value* = 1e-7. In the case of RNA Pol II ChIP, we used the peak caller SICER algorithm (9).

To associate peaks signals to genes, the *GeneMargin*, distance upstream and downstream of a gene that determines whether an interval is associated with that gene, was set up to 10,000 bp upstream or downstream of a gene.

Identification of Super-Enhancers. Enhancers for H3K27ac and Med1 were defined as regions with enrichment for these two marks. To identify clusters of enhancers, we used the Rank Ordering of Super-Enhancers software (ROSE) (10, 11). The MACS peaks identified were used as input for this algorithm which allows regions within 12.5kb of each other to be stitched together. The ROSE algorithm ranks all the enhancers by increasing total background-subtracted ChIP-seq signal of the co-factor, epigenetic mark, or transcription factor analyzed (x-axis) and plots the background-subtracted ChIP-seq occupancy in units of total reads per million per base pair (y-axis). An inflection point (geometrically defined) in the distribution of the occupancy of the factor is used to establish the cutoff for super-enhancers (10, 11). ROSE was run with a stitching distance of 12.5kb by default and without promoter exclusion.

Assay for Transposase Accessible Chromatin with high-throughput sequencing. ATAC-Seq was performed to identify open chromatin regions in juxtaglomerular cells, cells isolated from acutely and chronically recruited mice and in As4.1 cells. Briefly, a transposase inserts sequencing adapters into unprotected regions of DNA, thereby acting as a probe for measuring chromatin accessibility genome-wide. ATAC-Seq library preparations were performed as described (12, 13). We collected 50,000 cells for As4.1 and from chronically recruited mice, and 17,000 juxtaglomerular cells and cells from acutely recruited mice. Cells were washed with PBS and treated with Lysis Buffer. Then, cells were re-suspended in a transposition reaction mix (Illumina, cat # FC-121-1030) followed by DNA purification, before PCR amplification with 12 cycles with barcode primers (Illumina, cat # FC-121-1011). PCR products were purified with AmpureXP beads (Beckman Coulter, cat # A63881), and qPCR was performed to check for enrichment. Paired-end ATAC-Seq libraries were sequenced by HudsonAlpha Institute for Biotechnology, Huntsville, AL. Peaks identified using the MACS2 peak caller with a q value threshold of 0.01, were merged with *DiffBind*. Coverage values were calculated using *bedtools multicov*. In short, the coverage values were normalized using the estimate SizeFactors function from the *DESeq2* R package. Peaks with low coverage values (sum of all normalized read coverages less than 30) were filtered out, and then peaks were clustered by foldchanges. A table is set up where a value of 1 was attributed to a peak/sample combination if its mean coverage value was 2.5 fold higher than the other samples, and given a value of -1 if it was 2.5 fold lower than the other samples. Peaks with scores of 0 across this table were considered unchanged within the entire sample. Individual clusters were derived from different combinations of these values, and then similar clusters were merged based on plotting the z-scores of the coverage values using *pheatmap* R package. Ngs.plot.r package was used to plot the genome coverage heatmaps by supplying the config file with a single bam from a representative replicate for each sample and then supplying a bed file containing the peaks in the same order in which the heatmap was generated. Ngs.plot.r was run with 250 fragment length and 10,000 bp flanking region, with local color scale and a reduce ratio of 5. ex. (ngs.plot.r -G mm10 -R bed -C name_of_config_file -GO none -FL 250 -L 10000 -SC local -P 0 -O name_of_result -RR 5). The pie chart was generated by first feeding the combined peaks file to HOMER's annotatepeaks.pl<http://annotatepeaks.pl> to derive annotations. Annotations that labeled as 5'-UTR, 3'-UTR, exon, intron, and TES are changed to "intragenic." The pie chart was plotted using the pie function in R with the values from the table function in the annotation column.

RNA-Seq. As4.1 cells were grown to a final count of $1{,}5x10^7$ cells and fixed according to the manufacturer protocol. The sample was sent to Active Motif (Carlsbad, CA) to perform RNA isolation, library preparation, sequencing and initial data analysis. For As4.1 cells, 51.8 million read-pairs (75 nt) were used in the analysis. The TopHat v2.0.10 algorithm (*http://ccb.jhu.edu/software/tophat/manual.shtml*) was used to align the reads to the mm10 genome, and 39 million aligned pairs were found. The alignments in the BAM file were further analyzed using Cufflinks v.2.2.0 (*http://cole-trapnell-lab.github.io/cufflinks/manual/*). Cufflinks was run using the mm10-genes as a reference database (gtf file). By doing so, the output shows the known genes with their RNA-Seq metrics (as FPKM = Fragments Per Kilobase of exon model per Million mapped fragments).

For renin cells isolated from *Ren1*$^{c\text{-}YFP}$ mice, the Clontech SMARTer-Seq Lysis, RT, and PCR solutions (Mountain View, CA; Catalog No. 634833) were used to generate bulk cDNA samples (~400 cells from the resuspended cells post-FACS). The cDNA was diluted with Fluidigm dilution buffer the following day and stored at -20°C. The samples were quantified using a Qubit 3.0 Fluorometer (Thermo Fisher Scientific, Waltham, MA). Samples underwent next-generation sequencing library preparation as described in the Fluidigm C1 manual using an Illumina NexteraXT library prep and index kits (Catalog Nos. FC-131-1096 and FC-131-1002). Briefly, cDNA samples were diluted, tagmented, and indexed with unique barcodes for downstream

analyses. After the addition of indices and amplification, samples were multiplexed and cleaned using AMPure beads. All samples were sequenced on a HiSeq2500/4000 platform through the Beijing Genomics Institute (Shenzhen, Guangdong, China).

We used FastQC to assess the quality of FASTQ file reads. Prior to alignment, we removed low quality reads and adapter sequences using Trimmomatic0.36 (14, 15). We aligned FASTQ reads to the GRCm38/ENSEMBL mouse genome using Salmon0.7.2 with --gcBias and --seqBias optional flags (16, 17). Samples with less than 300,000 total aligned reads were excluded from downstream analyses. Transcript-level estimates of expression were scaled up to gene level estimates using the *Tximport* 1.2.0 R package, with the "lengthScaledTPM" argument for abundance estimation (18).

The data discussed in this publication have been deposited in NCBI's GEO and are accessible through GEO Series accession number GSE117725.

Ngs.plots. The '*ngs.plot.r'* program of the ngsplots package (19) was used to plot the average density of ChIP-Seq signal in the region of the transcription start site (TSS) of all genes in the mouse mm10 genome assembly. The input for each plot was sorted and indexed BAM files were produced by mapping the ChIP-Seq reads to the genome. BAM files for ChIP-Seq were those provided by Active Motif. For ATAC-Seq they were generated by mapping reads in fastq files to the mm10 genome using *Bowtie2* (reformatting SAM file to BAM using *samtools*).

CRISPR/Cas9 system. Cells were transfected transiently with the multiplex plasmid generated according to Yamamoto T. et al. (20). To construct the multiplex CRISPR/Cas9 vectors we used the CRISPR kit from Takashi Yamamoto(Addgene #1000000054, Hiroshima University, Hiroshima, Japan).

Target recognition requires a sgRNA sequence complementary to the genomic DNA and the presence of an NGG sequence (protospacer adjacent motif, PAM) at the 3′ end of the target site. To delete the classic *Renin* enhancer and the Rbpj-Enhancer we placed the sgRNAs at the 5' end and +50bp to the 3' end of the CE (320bp), and 5' and 3' of the 119 bp region of the *Rbp-j* Enh. The average transfection efficiency achieved was ~60% as evidenced by the presence of GFP+ cells in the cultures (Figure S4) and there was no difference in cell growth between transfections. After sorting for GFP+, cells we isolated DNA and RNA to determine the presence of the deletions and to measure *Renin* expression levels, respectively. Sanger sequencing of PCR products confirmed that the deletions of the CE and the *Rbpj* Enh occurred as predicted. The sgRNAs were designed using CRISPR Design tool developed by Fen Zhang at MIT; the sequences are listed in Table S11. We transfected the cells using the 4D-Nucleofector™ System (Lonza). The cells were incubated for 48h and pictures were taken. The supernatant was kept at -80°C to measure renin by ELISA and cells were trypsinized and resuspended to be sorted on behalf of eGFP expression.

For CRISPR/dCas9p300 experiments, five sgRNAs targeting the super-enhancer region of *Renin* were first cloned in a multiplex plasmid as mentioned above. The sequences of the sgRNA are shown in Table S11. Subsequently the Cas9 sequence was replaced by the dCas9p300 sequence from plasmid pcDNA-dCas9-p300 Core (Addgene# 61357; deposited by Charles Gersbach, Duke University, Durham, NC). $SMC^{CFP/YFP}$ were transfected by nucleofection (Lonza) according to the manufacturer's instructions. Cells were analyzed for YFP and renin expression 72h after transfection. YFP+ cells were imaged using a Leica DMIRE2 fluorescence microscope.

Histological and immunohistochemical analysis. Mice were anesthetized with tribromoethanol (300 mg/kg). Kidneys were harvested at indicated time points, weighed, fixed overnight in Bouin's fixative, and embedded in paraffin. Sections (5 μm) were deparaffinized in xylenes and graded alcohols and stained with hematoxylin and eosin to examine overall kidney morphology and Masson's Trichrome to identify areas of fibrosis as described previously (Gomez et al. 2009;

Sequeira-Lopez et al. 2010). We performed immunohistochemistry for renin (1:500 dilution of rabbit polyclonal anti-mouse antibody) to determine the distribution of renin-expressing cells and α-smooth muscle actin (SMA, 1: 10,000 dilution of mouse monoclonal antibody; Sigma, St. Louis, MO) to evaluate vascular architecture, as described previously (21, 22).
The juxtaglomerular apparatus (JGA) index was calculated as the number of renin-positive JGA per total number of glomeruli and expressed as a percentage. To determine the length of renin staining, we measured the maximal length of each renin-staining JGA.

RNA extraction and Quantitative Real-Time PCR. Whole kidneys from control and mutant animals were removed and placed in RNA*later* (Ambion, Austin, TX) overnight at 4°C and then stored at −20°C. Total RNA was isolated using Trizol extraction (Life Technologies, Grand Island, NY) according to the manufacturer's instructions. cDNA was prepared from 3 *μ*g of RNA using Maloney murine leukemia virus reverse transcriptase (Promega) and an oligo(dT) primer according to the manufacturer's instructions. Quantitative reverse transcription polymerase chain reaction (RT-PCR) was performed using SYBR Green I (Invitrogen Molecular Probes, Eugene, OR) in a CFX Connect system (BioRad, Hercules, CA). *Ren1*, *Med1* and *Akr1b7* mRNA expression were normalized to *S14* expression, and the changes in expression were determined by the ΔΔCt method and are reported as relative expression compared to control mice. The following gene-specific primers were used: *Ren1*, forward, 5'-ACAGTATCCCAACAGGAGAGACAAG-3', reverse, 5'-GCACCCAGGACCCAGACA -3'; Med1, forward, 5'-GTTCTGGAGGGCATCAGCAT-3', reverse, 5'-GGTGAGAGCCCAGTCCATTC-3'; Akr1b7, forward, 5'- CCTGTTGGATGCAAGGACTGA-3', reverse, 5'-CCTGCATTGCCAGATGGTAG-3'; *S14*, forward, 5'-CAGGACCAAGACCCCTGGA-3', reverse 5'-ATCTTCATCCCAGAGCGAGC-3'.

Blood Pressure Measurement. Mice were anesthetized with 1.5% isoflurane and placed on a thermostatically controlled heating table at 37.5°C. A polyethylene catheter (Becton Dickinson) pre-filled with heparinized saline was inserted into the right carotid so that the catheter tip lied at the aortic root. Mean arterial pressure was continuously recorded from this catheter by means of an RX104A transducer coupled to a data acquisition system and AcqKnowledge software (Biopac systems, Inc.). Measurements of mean arterial pressure, systolic and diastolic blood pressure were taken over a 10-min period (23, 24). Animals were euthanized after the procedure.

Acute Recruitment Study. Ren1^{cYFP} mice at two months of age were treated with Low Sodium Diet (0.1%, 7034, ENVIGO, Madison, WI) plus Captopril added to the drinking water (0.5 g/L) for seven days (25, 26). At the end of the treatment period, YFP+ cells were isolated by FACS and cells were used to perform ATAC-Seq.

Blood Chemistry. Blood was collected by cardiac puncture or through the carotid catheter when mice were subjected to blood pressure measurement. After blood was collected for renin measurements, blood samples were collected into heparinized and EDTA plasma separator tubes (Microtainer). Complete blood count and the basic metabolic panel were performed by the University of Virginia Hospital clinical laboratory (7).

Plasma renin. Plasma RENIN concentration was determined using ELISA following the manufacturer's instructions (RayBiotech, Norcross, GA) (27).

Statistics. Statistical parameters are reported in the figures and figure legends. Results statistically significant were obtained when $p < 0.05$ by two-tailed Student's t-test. Statistical analysis was performed in GraphPad Prism 7. Wilcoxon Signed-Rank Test a non-parametric test

used to compare samples not normally distributed and to assess whether their population mean ranks differed.

References.

1. Sigmund CD et al. Isolation and characterization of renin-expressing cell lines from transgenic mice containing a renin-promoter viral oncogene fusion construct. [Internet]. *J. Biol. Chem.* 1990;265(32):19916–19922.
2. Pentz ES, Lopez MLSS, Cordaillat M, Gomez RA. Identity of the renin cell is mediated by cAMP and chromatin remodeling: an in vitro model for studying cell recruitment and plasticity. [Internet]. *Am. J. Physiol. Heart Circ. Physiol.* 2008;294(2):H699-707.
3. Takahashi N et al. Ren1c Homozygous Null Mice Are Hypotensive and Polyuric, but Heterozygotes Are Indistinguishable from Wild-Type [Internet]. *J. Am. Soc. Nephrol.* 2005;16(1):125–132.
4. Jia Y et al. Transcription Coactivator PBP, the Peroxisome Proliferator-activated Receptor (PPAR)-binding Protein, Is Required for PPARα-regulated Gene Expression in Liver [Internet]. *J. Biol. Chem.* 2004;279(23):24427–24434.
5. Sequeira López MLS, Pentz ES, Nomasa T, Smithies O, Gomez RA. Renin cells are precursors for multiple cell types that switch to the renin phenotype when homeostasis is threatened. *Dev. Cell* 2004;6(5):719–728.
6. Matsumoto K et al. Transcription coactivator PBP/MED1-deficient hepatocytes are not susceptible to diethylnitrosamine-induced hepatocarcinogenesis in the mouse [Internet]. *Carcinogenesis* 2010;31(2):318–325.
7. Oka M, Medrano S, Sequeira-López MLS, Gómez RA. Chronic Stimulation of Renin Cells Leads to Vascular Pathology [Internet]. *Hypertension* 2017;70(1):119 LP-128.
8. Zhang Y et al. Model-based Analysis of ChIP-Seq (MACS) [Internet]. *Genome Biol.* 2008;9(9):R137–R137.
9. Zang C et al. A clustering approach for identification of enriched domains from histone modification ChIP-Seq data [Internet]. *Bioinformatics* 2009;25(15):1952–1958.
10. Whyte WA et al. Master transcription factors and mediator establish super-enhancers at key cell identity genes. *Cell* 2013;153(2):307–319.
11. Lovén J et al. Selective inhibition of tumor oncogenes by disruption of super-enhancers. [Internet]. *Cell* 2013;153(2):320–34.
12. Buenrostro JD, Giresi PG, Zaba LC, Chang HY, Greenleaf WJ. Transposition of native chromatin for fast and sensitive epigenomic profiling of open chromatin, DNA-binding proteins and nucleosome position [Internet]. *Nat. Methods* 2013;10:1213.
13. Buenrostro J, Wu B, Chang H, Greenleaf W. ATAC-seq: A Method for Assaying Chromatin Accessibility Genome-Wide [Internet]. *Curr. Protoc. Mol. Biol.* 2015;109:21.29.1-21.29.9.
14. Andrews S. FastQC: a quality control tool for high throughput sequence data. [Internet]2010;http://www.bioinformatics.babraham.ac.uk/projects/fastqc/. cited
15. Bolger AM, Lohse M, Usadel B. Trimmomatic: a flexible trimmer for Illumina sequence data [Internet]. *Bioinformatics* 2014;30(15):2114–2120.
16. Patro R, Duggal G, Love MI, Irizarry RA, Kingsford C. Salmon provides fast and bias-aware quantification of transcript expression [Internet]. *Nat. Methods* 2017;14:417.
17. Aken BL et al. The Ensembl gene annotation system [Internet]. *Database J. Biol. Databases Curation* 2016;2016:baw093.
18. Soneson C, Love MI, Robinson MD. Differential analyses for RNA-seq: transcript-level estimates improve gene-level inferences [version 1; referees: 2 approved] [Internet]. *F1000Research* 2015;4(1521). doi:10.12688/f1000research.7563.1
19. Shen L, Shao N, Liu X, Nestler E. ngs.plot: Quick mining and visualization of next-generation sequencing data by integrating genomic databases [Internet]. *BMC Genomics*

2014;15:284.
20. Sakuma T, Nishikawa A, Kume S, Chayama K, Yamamoto T. Multiplex genome engineering in human cells using all-in-one CRISPR/Cas9 vector system [Internet]. *Sci. Rep.* 2014;4:5400.
21. Sequeira Lopez ML, Pentz ES, Robert B, Abrahamson DR, Gomez RA. Embryonic origin and lineage of juxtaglomerular cells. [Internet]. *Am. J. Physiol. Renal Physiol.* 2001;281(2):F345-56.
22. Lin EE, Sequeira-Lopez MLS, Gomez RA. RBP-J in FOXD1+ renal stromal progenitors is crucial for the proper development and assembly of the kidney vasculature and glomerular mesangial cells [Internet]. *Am. J. Physiol. - Ren. Physiol.* 2014;306(2):F249–F258.
23. Pentz ES, Moyano MA, Thornhill BA, Sequeira Lopez MLS, Gomez RA. Ablation of renin-expressing juxtaglomerular cells results in a distinct kidney phenotype [Internet]. *Am. J. Physiol. Integr. Comp. Physiol.* 2004;286(3):R474–R483.
24. Pentz ES et al. Ren1d and Ren2 cooperate to preserve homeostasis: evidence from mice expressing GFP in place of Ren1d [Internet]. *Physiol. Genomics* 2001;6(1):45–55.
25. Castellanos Rivera RM et al. Transcriptional regulator RBP-J regulates the number and plasticity of renin cells. [Internet]. *Physiol. Genomics* 2011;43(17):1021–8.
26. Castellanos-Rivera RM et al. Recombination signal binding protein for Ig-κJ region regulates juxtaglomerular cell phenotype by activating the myo-endocrine program and suppressing ectopic gene expression. [Internet]. *J. Am. Soc. Nephrol.* 2015;26(1):67–80.
27. Belyea BC et al. Identification of renin progenitors in the mouse bone marrow that give rise to B-cell leukaemia [Internet]. *Nat. Commun.* 2014;5:3273.

Supplemental Figures.

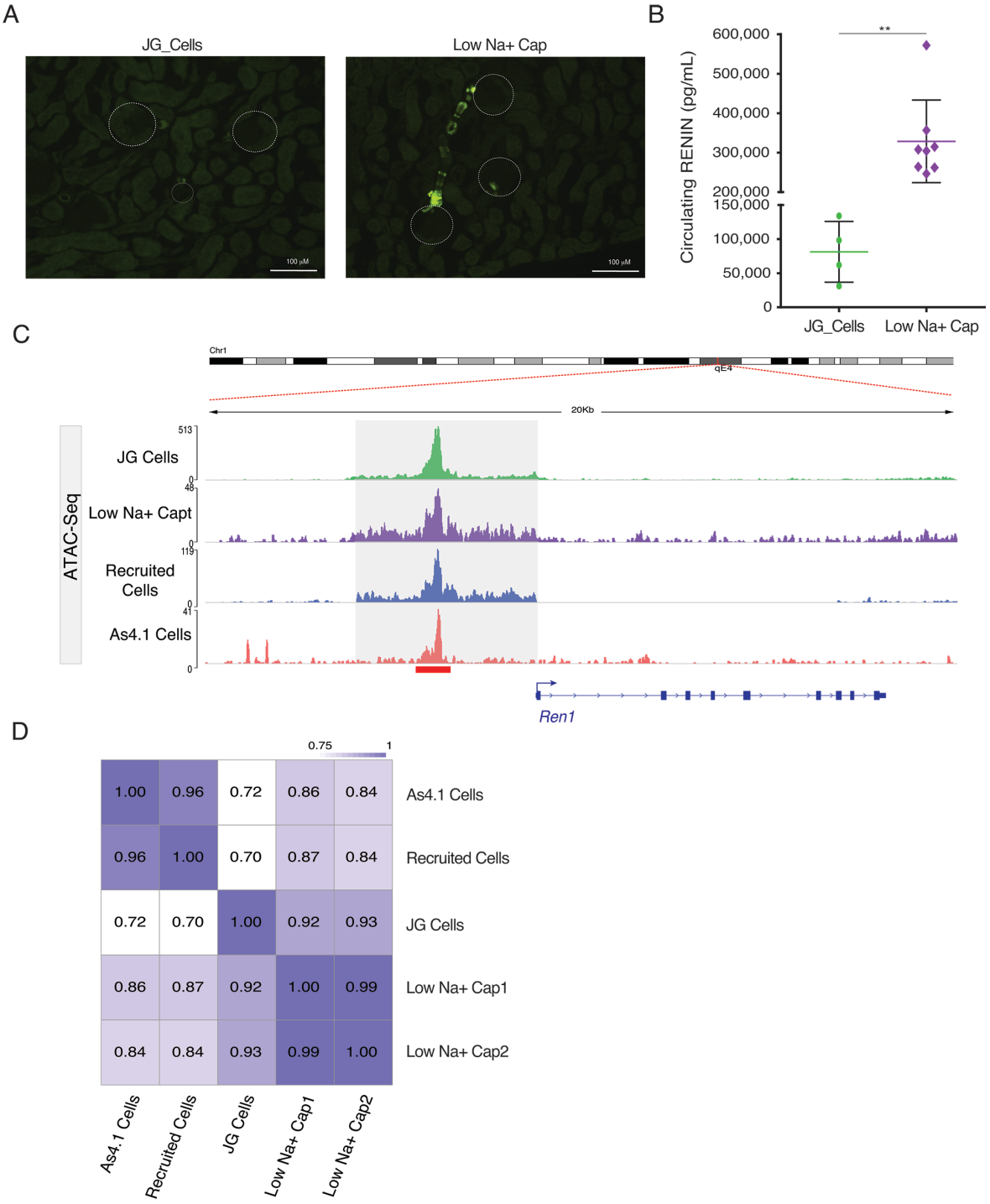

Supplemental Figure 1. Renin cells possess a distinguishing pattern of chromatin accessible at the renin locus. A. Left. Kidney section from a *Ren1*$^{c\text{-}YFP}$ wild type mouse (n=8). In this mouse YFP expression is driven by the renin promoter thus marking the JG renin expressing cells. The YFP signal is restricted to the juxtaglomerular cells at the entrance to the glomerulus. Right. Kidney section from a *Ren1*$^{c\text{-}YFP}$ mouse treated with Low Na^+ diet (0.1%) plus Captopril (0.5g/L) added to the drinking water for seven days

(n=8). YFP+ cells reporting the activity of the renin promoter are distributed along the afferent arterioles, at the entrance to the glomerulus and in the mesangium. These cells are distributed in a similar pattern to the chronically stimulated (recruited) renin cells mentioned in Figure 1B. B. Plasma RENIN levels are significantly higher in acutely recruited mice (n=8; untreated, n=4). C. Genome browser image at the renin locus shows a notable similar pattern of accessible chromatin among the four renin cell types studied: JG cells, Low Na + Cap, chronically stimulated (recruited) cells and As4.1 cells. D. Heatmap showing the Pearson correlation coefficients between the ATAC-Seq peak scores for each sample. A higher score and darker color indicates a greater degree of similarity between the ATAC-Seq profiles of the two samples being compared denoted by the row and column pertaining to that score. In B, data are presented as mean ± SD. Statistical significance between two groups was determined by unpaired Student's *t*-test. A p value ≤0.01 was considered significant.

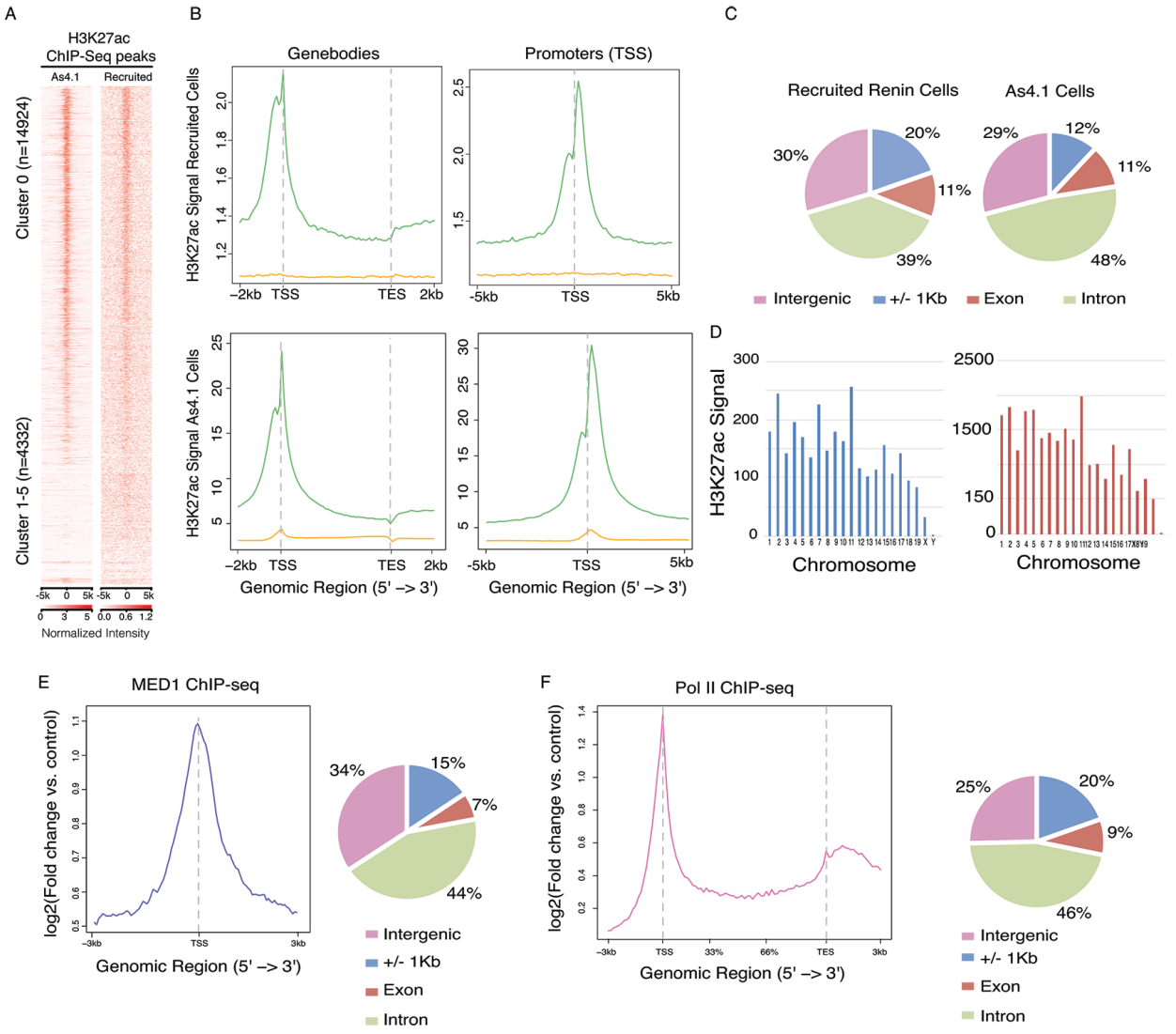

Supplemental Figure 2. Genome-wide distribution of H3K27ac signal in recruited renin cells as well as in As4.1 cells, and distribution of MED1 and Pol II along the genome of As4.1 cells. A. Heatmap depicts the sequencing read coverage intensity for H3K27ac in As4.1 and recruited renin cells at 19256 consensus ATAC-Seq peaks identified in the three renin cell types (See Figure 2). B. Left. Average plots of ChIP-Seq signal for H3K27ac showing its distribution across gene bodies (left) in the range of -2kb upstream the transcription start site (TSS) to +2kb downstream the transcription end site (TES). Right. H3K27ac signal distribution at promoter locations across the genome in the range of -5Kb to +5Kb from the (TSS). Top. Recruited cells. Bottom, As4.1 cells. Orange: ChIP-Seq input. C. Pie chart showing the distribution of enhancer elements in the genome of recruited renin cells (left) and As4.1 cells (right). D. Genomic distribution of H3K27Ac peaks across the chromosomes of recruited renin cells (left) and As4.1 cells (right). E. MED1 intensity coverage (left) along genomic regions of As4.1 cells located -3Kb

to +3Kb from the (TSS). Right. Pie chart shows the distribution of MED1 across the genome. F. Average plot for Pol II shows a high signal intensity at the TSS and its occupancy along the gene body to the TES of the genes. Pie chart shows the distribution of MED1 across the genome. Genomic regions in x-axis and values in log scale in y-axis.

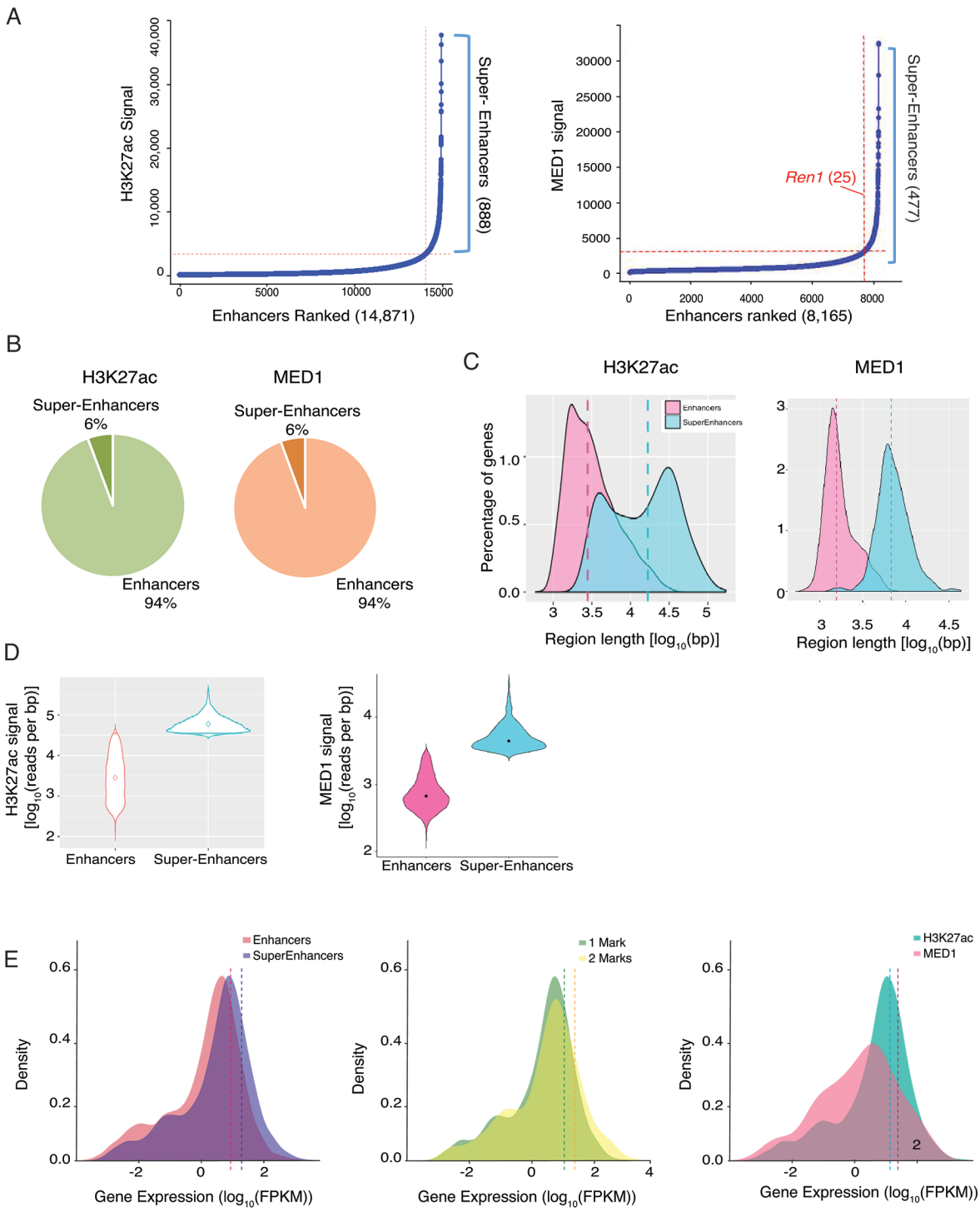

Supplemental Figure 3. Super-enhancers in As4.1 cells. A. Left. Hockey plot depicting the 888 super-enhancers identified based on H3K27Ac enrichment across the enhancers ranked. Right, MED 1 ChIP-Seq signal across the 8,165 enhancers in As4.1 cells; 477 super-enhancers were identified where *Ren1* gene is ranked at position 25**.** B. Pie charts illustrate the percentage of super-enhancers overlapping the H3K27ac (left) and MED1 (right) peaks in As4.1 cells. C.

Distribution histogram showing that super-enhancer regions in As4.1 cells are larger in length than typical enhancers in H3K27ac (left) and MED1 (right) ChIP-Seq. D. Violin plots shows that super-enhancers had more cumulative enrichment intensity than typical enhancers. E. Histograms showing differential expression between genes associated or not to super-enhancers. Left, comparison between genes associated (purple) and non- associated (pink) to super-enhancers. The curve for the group that has super-enhancers is shifted to the right showing that this group of genes are more highly expressed than the group without super-enhancers *(p= <2.2e-16)*. Middle, comparison between genes associated to one (green) or two (yellow) marks indicating super-enhancers. One super-enhancer means that could be associated to H3K27ac or MED1, while 2 super-enhancers involved the association of two marks. Right, comparison between genes associated to H3K27ac (green) or MED1 (pink). The histograms show on the y-axis the density of genes based on each expression range in a logarithmic scale, plotted on the x-axis. The dotted lines show the mean for each group of genes.

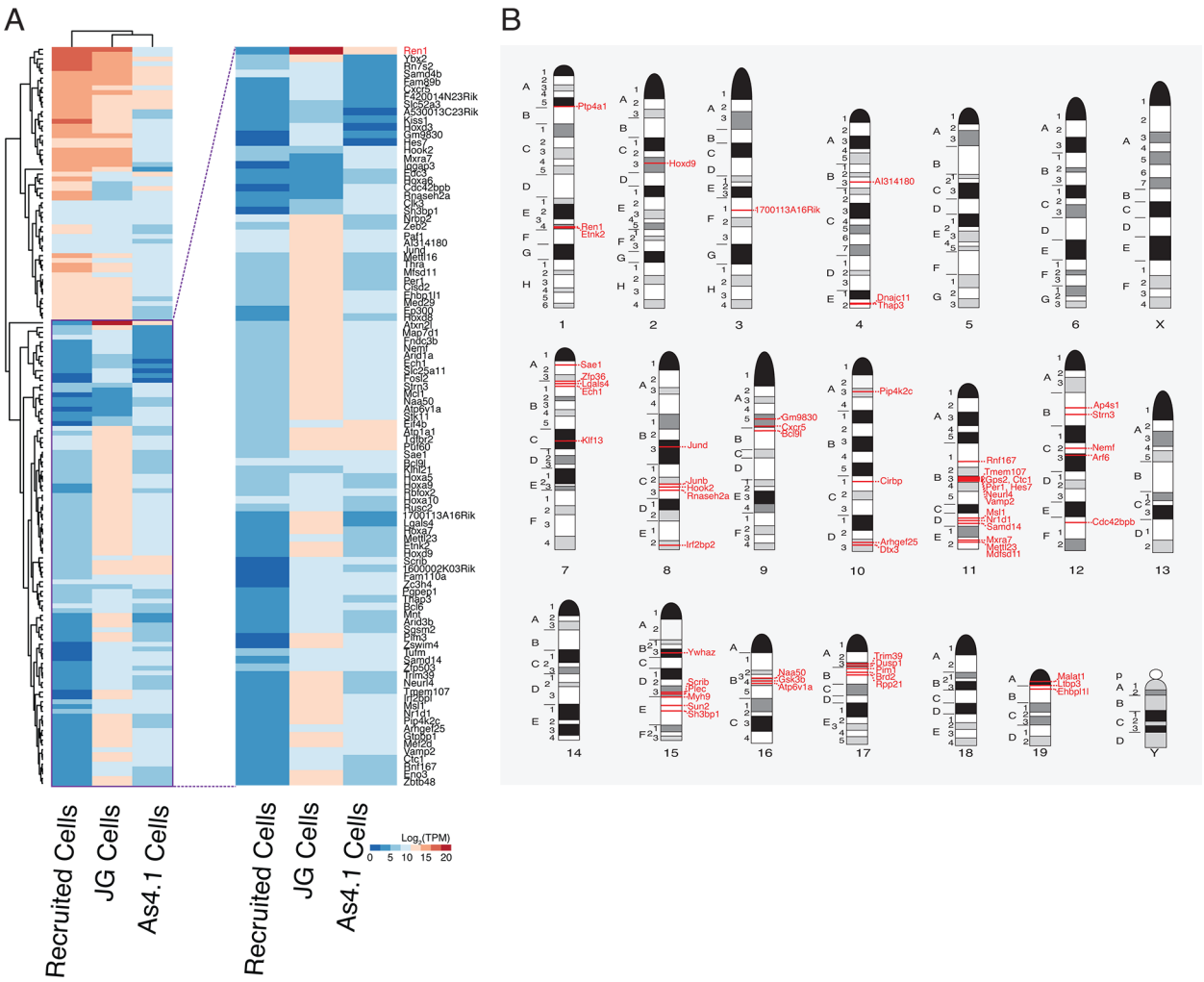

Supplemental Figure 4. Renin cells possess an exclusive set of super-enhancers associated genes involved in renin cell phenotype. A. Heatmap showing the level of expression for super-enhancer associated genes in the three cell types. Inset to the right enlarge the cluster of the renin gene, which shows the expected transcription level for each cell type (Juxtaglomerular cells: high; recruited cells: null; As4.1 cells: medium to high). B. Super-enhancer associated genes expressed in renin cells show a non-homogenous distribution along chromosomes.

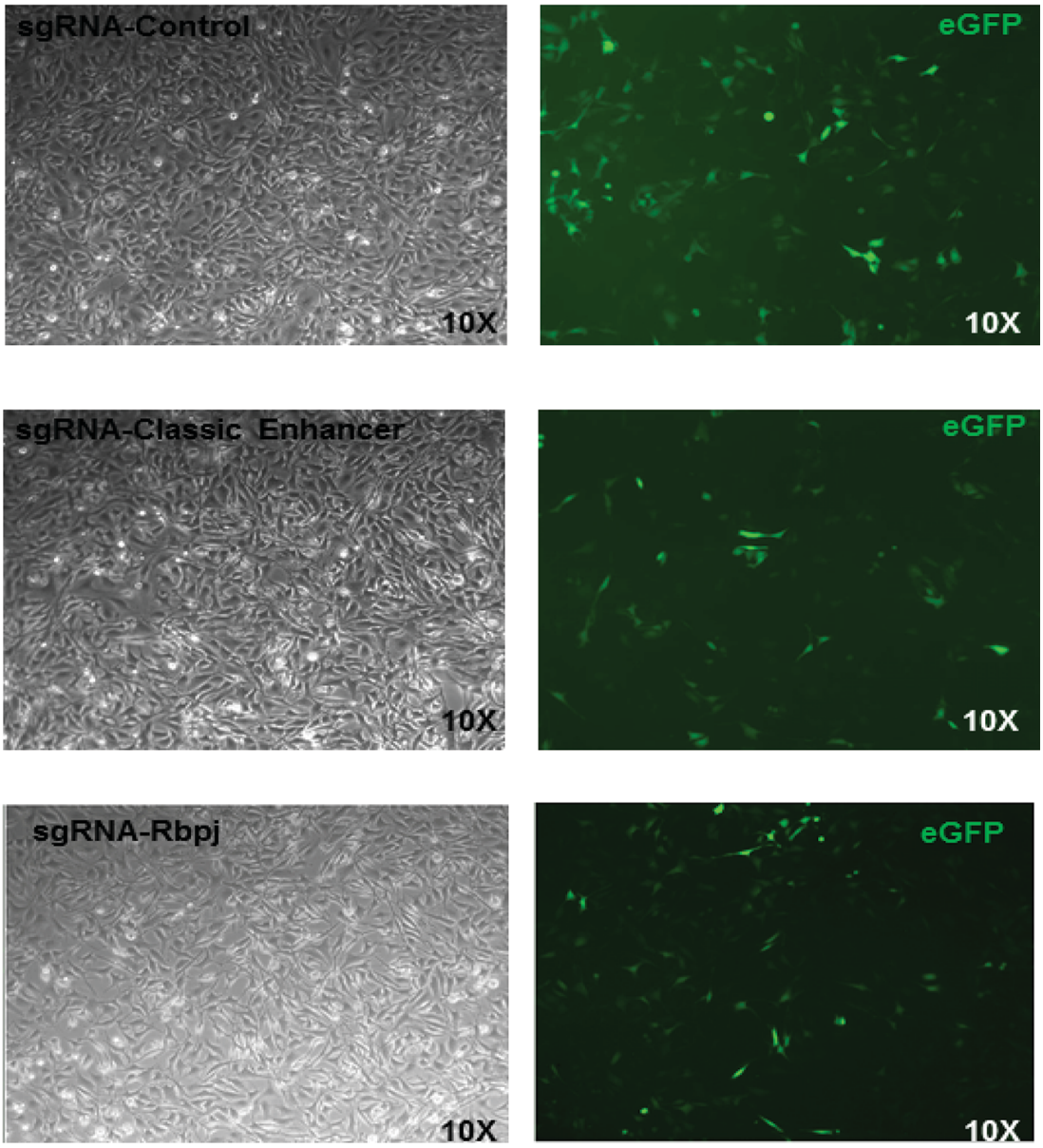

Supplemental Figure 5. As4.1 cells transfected with multiplex CRISPR-Cas9 plasmids. Microscope images show transfected cells with plasmids to delete regulatory elements at the renin super-enhancer region. Pictures were taken 48hs after transfection. Images to the right show that ~60% of the cells express eGFP indicating that transfection occurred.

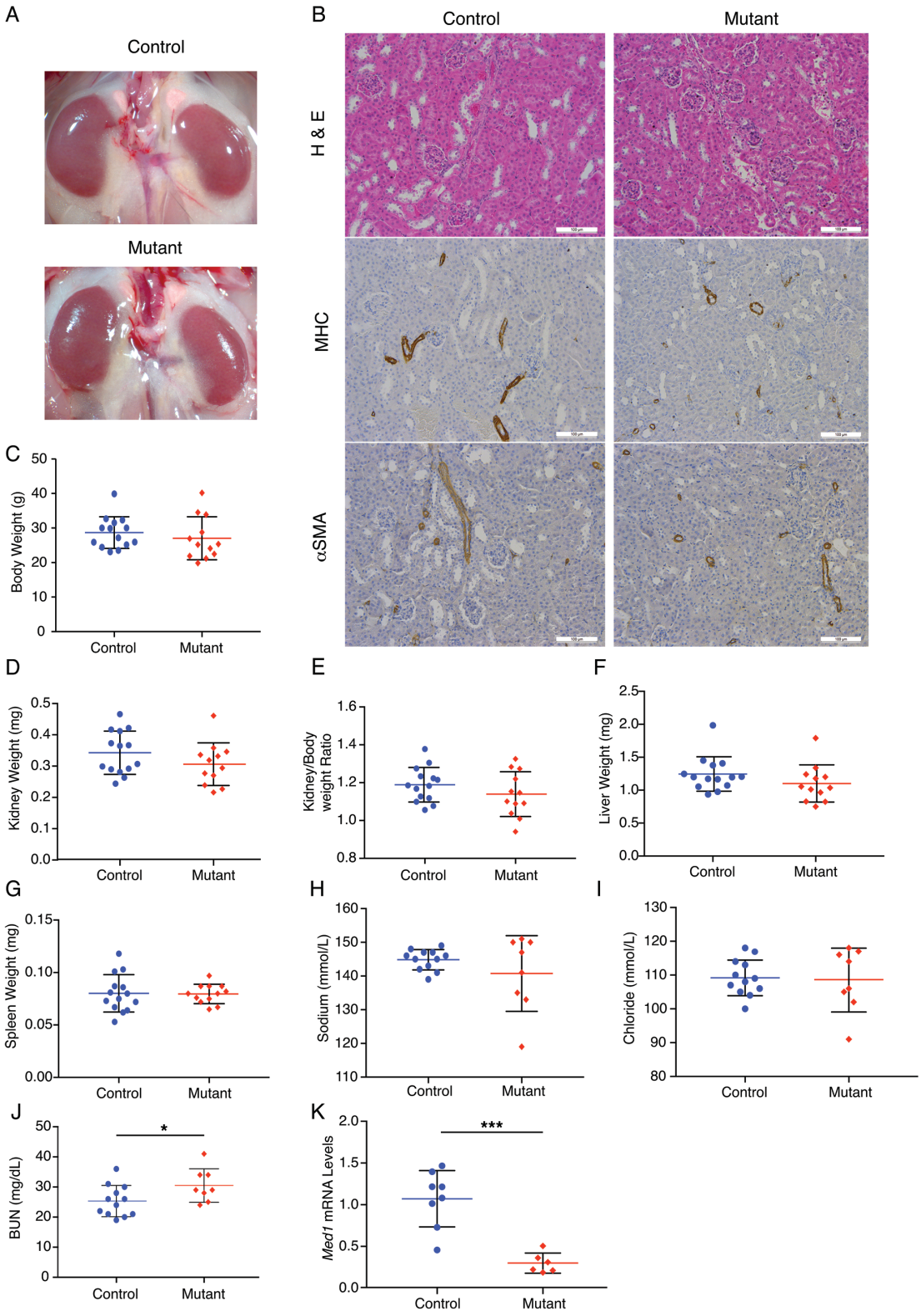

Supplemental Figure 6. Characterization of *Med1*$^{fl/-}$*; Ren1d*$^{Cre/+}$ mice. Kidneys of mutant mice do not show macroscopically differences (controls, n=14; mutants, n=12). B. H&E staining

(top), immunostaining for myosin heavy chain (middle) α-smooth muscle actin (α-SMA, bottom) did not reveal differences between mutant and control group suggesting that *Med1* it is not affecting kidney development (controls, n=8; mutants, n=6). *Med1* mutant mice did not show differences in body weight, kidney weight, kidney/body weight ratio, liver or spleen weight (D-G. Controls, n=14; mutants, n=12). Sodium and Chloride plasma levels were not different between groups (H-I). J. Significant elevated blood urea nitrogen in mutant mice indicates an early stage of renal insufficiency. For H-J, controls, n=12; mutants, n=8. K. *Med1* mRNA levels were decreased in mutants' mice compared to the control group (0.362 ± 0.145vs. 1.077 ± 0.478, $p<0.001$, indicating the lack of *Med1* in these mice (Controls, n=8; mutants, n=6). In J, data are presented as mean ± SD. Statistical significance between two groups was determined by unpaired Student's *t*-test. A p value ≤0.05 was considered significant.

Table S1. Regulatory regions identified in renin cells by ATAC-Seq.

Table S2. Genes expressed in renin cells characterized by open chromatin and H3K27ac deposition.

Table S3. 211 super-enhancers were identified in native renin cells according to H3K27ac enrichment.

Table S4. Genes associated with the 91 super-enhancers shared between recruited native renin cell and As4.1 cells.

Table S5. GO terms and KEGG pathways enriched in recruited native renin cells considering the 91 exclusive super-enhancers for this cell type.

Table S6. Genes from cAMP and Notch GO terms utilized for GeneMANIA to construct networks. Functions obtained from GeneMANIA and UniProt databases.

Table S7. List of transcription factors with putative binding sites along -5kb upstream to the start site of the renin gene.

Table S8. Transcription factors expressed in native renin cells with predicted binding sites in renin super-enhancer region.

Table S9. Transcription factors expressed in native renin cells that possess super-enhancer associated, and with predicted binding sites in the renin super-enhancer.
Values are expressed in Transcript per Millions.

Table S10. Oligonucleotides used for insertion of sgRNA target sequences. Related to
(Bold: sgRNA; underline: restriction enzyme site; F: forward; R; reverse; SE: super-enhancer; CE: classic enhancer)